Iron–Sulfur Cluster Biosynthesis in Algae with Complex Plastids

Christopher Grosche[1,2], Angelika Diehl[1,3], Stefan A. Rensing[2], and Uwe G. Maier[1,3,*]

[1]LOEWE Center for Synthetic Microbiology (Synmikro), Marburg, Germany

[2]Plant Cell Biology, Philipps University Marburg, Marburg, Germany

[3]Laboratory for Cell Biology, Philipps University Marburg, Marburg, Germany

*Corresponding author: E-mail: maier@staff.uni-marburg.de.

Abstract

Plastids surrounded by four membranes harbor a special compartment between the outer and inner plastid membrane pair, the so-called periplastidal compartment (PPC). This cellular structure is usually presumed to be the reduced cytoplasm of a eukaryotic phototrophic endosymbiont, which was integrated into a host cell and streamlined into a plastid with a complex membrane structure. Up to date, no mitochondrion or mitochondrion-related organelle has been identified in the PPC of any representative. However, two prominent groups, the cryptophytes and the chlorarachniophytes, still harbor a reduced cell nucleus of symbiont origin, the nucleomorph, in their PPCs. Generally, many cytoplasmic and nucleus-located eukaryotic proteins need an iron–sulfur cofactor for their functionality. Beside some exceptions, their synthesis is depending on a so-called iron–sulfur complex (ISC) assembly machinery located in the mitochondrion. This machinery provides the cytoplasm with a still unknown sulfur component, which is then converted into iron–sulfur clusters via a cytosolic iron–sulfur protein assembly (CIA) machinery. Here, we investigated if a CIA machinery is present in mitochondrion-lacking PPCs. By using bioinformatic screens and in vivo-localizations of candidate proteins, we show that the presence of a PPC-specific CIA machinery correlates with the presence of a nucleomorph. Phylogenetic analyses of PPC- and host specific CIA components additionally indicate a complex evolution of the CIA machineries in organisms having plastids surrounded by four membranes.

Key words: iron–sulfur cluster, cytosolic iron–sulfur protein assembly (CIA), periplastidal compartment, *Guillardia theta*, *Bigelowiella natans*, *Phaeodactylum tricornutum*.

Introduction

Cryptophytes and chlorarachniophytes, both eukaryotic phototrophic unicellular organisms, provide extraordinary examples in respect to the cellular minimization of a previously free-living organism. By merging two eukaryotic cells, a phototrophic symbiont was reduced within a host cell to a complex organized plastid surrounded by four membranes. Extraordinary minimization can be observed by the presence of a remnant cytoplasm of the eukaryotic symbiont, which is located between the outer and inner plastid membrane pair (Maier et al. 2015). In cryptophytes and chlorarachniophytes, this remnant cytoplasm (periplastidal compartment [PPC]) harbors a tiny cell nucleus, as the only well-defined PPC-located compartment (Grosche et al. 2014). This so-called nucleomorph is reduced in coding capacity as well as overall size (Douglas et al. 2001; Gilson et al. 2006;

Tanifuji et al. 2011; Moore et al. 2012; Tanifuji et al. 2014a; Suzuki et al. 2015). Although being, as mentioned, reduced, (e.g., Moore and Archibald 2009; Grosche et al. 2014), nucleomorphs are functional in respect to transcription and RNA processing (Tanifuji et al. 2014b; Suzuki et al. 2016), and the nucleomorph-encoded proteins are expected to be translated at PPC-specific 80S ribosomes. Thus, cryptophytes and chlorarachniophytes are unicellular organisms with two different cell nuclei located in two different eukaryotic cytoplasms, each one containing its own type of 80S ribosomes. However, many phylogenetically related organisms, such as diatoms, minimized their PPC more drastically, as here a nucleomorph and a second set of ribosomes are absent (Hempel et al. 2007; Bolte et al. 2009).

Assembly of ribosomes is highly coordinated (Maier et al. 2013) and requires, besides components present in mature

ribosomes, several accessory factors. One of these, the iron–sulfur cluster (Fe–S) containing protein Rli1, is involved in ribosome biogenesis in addition to translation initiation and termination (Kispal et al. 2005; Strunk et al. 2012). A central cellular role of Rli1 in this process can also be deduced from the fact that homologs are present in archaea and eukaryotes (Nurenberg and Tampe 2013). Accordingly, the presence of a gene encoding the Fe–S cluster protein Rli1-homolog in the nucleomorph of cryptophytes is not surprising (first identified by Douglas et al. 2001; but, as a member of ATP binding cassette [ABC] ATPases protein family, annotated as an ABC transporter). Nevertheless, the need for factors taking part in ribosome functions might be different in chlorarachniophytes, as neither a nucleomorph- nor a nucleus-encoded PPC-located Rli1 has yet been identified in silico. However, more likely Rli1 might be encoded in two versions in chlorarachniophytes as well, but the genes are not detectable in the genome sequence of *B. natans*. In any case, the presence of a RLI1 gene encoded by the cryptophyte nucleomorph demands Fe–S clusters to be present in the PPC of at least cryptophytes.

One of the major cell biological highlights of the last decades was the finding that typical aerobic eukaryotes depend on mitochondria for the synthesis of Fe–S clusters (see: Lill et al. 2014, 2015; Mühlenhoff et al. 2015). This makes mitochondria essential for the maturation of all cellular Fe–S proteins except for those of plastids, which possess a SUF (sulfur formation)-system (Balk and Pilon 2011; Lill et al. 2012). In the mitochondrion, Fe–S clusters are synthesized via the ISC assembly machinery, which also generates an essential sulfur component indispensable for cytosolic and nuclear Fe–S cluster assembly. This component is transported via the ABC transporter Atm1 (yeast, Atm3/Starik1 in *Arabidopsis*) into the cytoplasm (Kispal et al. 1999; Kushnir et al. 2001; Bernard et al. 2009; Lill et al. 2014). Due to its so far unknown nature this component is referred to as X-S (Lill et al. 2015). In the cytoplasm X-S, together with monothiol glutaredoxins, is processed by a so-called cytosolic iron–sulfur protein assembly (CIA) machinery to generate cytosolic and nuclear Fe–S proteins (Netz et al. 2014). Most components of both the ISC- and CIA-machineries are generally essential for aerobic eukaryotes and defects therefore affect the whole cell leading to so-called Fe–S diseases (Stehling et al. 2014).

Since at least the genetically active PPC of cryptophytes seems to require Fe–S clusters a mitochondrion or mitochondrion-related organelle providing the Fe–S clusters (MRO, e.g., Makiuchi and Nozaki 2014) would be expected. However, no such organelle could be identified in the PPC on the ultrastructural level so far. If correct, Fe–S clusters for PPC proteins are either synthesized by another PPC-specific machinery, or X-S components or Fe–S clusters have to be imported into the PPC. Especially for the latter, at least remnants of a CIA machinery (Lill et al. 2015) for the assembling of PPC-specific Fe–S proteins might be present.

In order to search for the here postulated PPC-specific CIA machineries, we screened the genomes of a cryptophyte, a chlorarachniophyte and a diatom for putative CIA factors. Our results suggest that, in parallel to a CIA machinery in the host cytoplasm, PPC-specific CIA factors are encoded in the genomes of cryptophytes and most likely chlorarachniophytes, whereas diatoms lack a PPC-specific CIA machinery. Our phylogenetic studies on the central CIA factors Cfd1 and Nbp35 (both are central P-loop NTPases serving as scaffold proteins for cytosolic iron–sulfur protein assembly) indicated different origins of host- and symbiont-specific Nbp35 proteins in cryptophytes, chlorarachniophytes and the host version of diatoms. Moreover, the presence of Cfd1, generally not known from members of the SAR supergroup (Stramenopiles, Alveolates and Rhizaria), was confirmed for a host version for cryptophytes (Tsaousis et al. 2014). As a PPC-version of a mitochondrion or a MRO was never identified in cryptophytes, we finally hypothesize that a X-S component for ISC assembly in the PPC of cryptophytes is supplied by the plastid SUF system and imported into the PPC.

Materials and Methods

Culture Conditions

Phaeodactylum tricornutum was cultivated in f/2 medium (Guillard 1975), adjusted to pH 7.2, under constant illumination (80 µmol photons·m^{-2}·s^{-1}) at 22 °C. Liquid cultures were grown with agitation (150 rpm) in a volume of 300 ml.

Guillardia theta was cultured in h/2 medium, a modified f/2 medium with a final NH$_4$Cl concentration of 500 µM, without agitation at 15 °C in a 12h/12h day/night cycle in a volume of 100–200 ml.

In silico Analyses and Factor Identification

Factors of the CIA machinery were identified using the known factors of *S. cerevisiae* in a reciprocal BLAST (Altschul et al. 1990) approach against the genomes of *B. natans*, *G. theta*, and *P. tricornutum* (Bowler et al. 2008; Curtis et al. 2012), the nucleomorph genomes of *B. natans* and *G. theta* were also included (Douglas et al. 2001; Gilson et al. 2006). Gene models of identified candidates were manually checked **for**, for example, EST or RNASeq coverage and analyzed for presence of N-terminal targeting signals using SignalP 3.0 (Bendtsen et al. 2004), TargetP 1.1 (Emanuelsson et al. 2000) and alignments of the N-terminus (supplementary fig. S1, Supplementary Material online). Cia1 and Cia2 candidates were analyzed with help of HmmerWeb Version 2.23.0 and Gene3D prediction (supplementary figs. S3 and S4, Supplementary Material online) (Finn et al. 2015; Dawson et al. 2017; Lewis et al. 2018; Potter et al. 2018).

Phylogenic Reconstruction

To verify ortholog status of identified factors, yeast and before (see above) identified query protein sequences were searched with BLASTP (Altschul et al. 1990) against a plant-specific, custom-made protein database that included genomes of the species listed in supplementary table S2, Supplementary Material online. Results were filtered according to Rost (1999) to keep homologous sequences only. Additionally, sequences for Nbp35 and Cfd1 were added from the results of Tsaousis (Tsaousis et al. 2014) and from a NCBI Blast to add additional sequences from especially SAR and fungal species (see supplementary table S2, Supplementary Material online). Resulting sequences were aligned using MUSCLE version v3.8.31 (Edgar 2004) in automatic mode, and resulting alignments were inspected manually, duplicated sequences were removed and alignment was trimmed using Jalview version 2.8 (Clamp et al. 2004). Based on these alignments, neighbor-joining (NJ) guide trees were built using quicktree_sd (http://hdl.handle.net/10013/epic.33164.d001; Last accessed March 27, 2018) with 1,000 bootstrap samples. Sequences with very long branches, potentially representing flawed gene models, were removed upon inspection of initial trees. Afterwards, the appropriate models were selected based on AIC/BIC using ProtTest 3.4 (Guindon and Gascuel 2003; Darriba et al. 2011). Final phylogenies were constructed by Bayesian inference (BI) using Mr. Bayes 3.2.5 (Ronquist et al. 2012). BI analysis was run with two hot and two cold chains, discarding 25% of trees as burn-in, for 8,000,000 generations (standard deviation of split frequencies 0.027225). The resulting tree was displayed, colored, and midpoint-rooted with FigTree version 1.4.2 (http://tree.bio.ed.ac.uk/software/figtree/; Last accessed March 27, 2018), schematic tree representation was done with iTOL (Letunic and Bork 2016).

In vivo Localizations of CIA Proteins

The sequences of PPC localized Dre2 (ProtID: 199508), Nar1 (ProtID: 138617), Nbp35 (ProtID: 186667), and Tah18 (ProtID: 198059) can be retrieved from the G. theta genome database (https://genome.jgi.doe.gov/Guith1/Guith1.home.html; Last accessed March 27, 2018). RNA was isolated from 100 ml culture of G. theta using a TRIzol (Thermo Scientific) protocol as described previously (Grosche et al. 2012), residual DNA was removed using DNAseI (Thermo Scientific) and RNA was precipitated using NaAc/EtOH precipitation after subsequent Phenol and Chloroform treatment. RNA was reverse-transcribed with RevertAid Premium RT (Thermo Scientific) using standard protocol according to manufacturer. Full-length sequences of all genes were amplified with standard PCR conditions using Phusion polymerase (Thermo Scientific) from G. theta cDNA. Primer used for amplification are shown in supplementary table S3, Supplementary Material online.

For heterologues in vivo localization studies in P. tricornutum, the amplicates were cloned 5′ to eGFP (5′-amplificate-eGFP-3′) into the nitrate inducible pPha-NR vector (GenBank: JN180663) after intermediate cloning into pJET vector (Thermo Scientific). Apart from Tah18 full length sequences were used for localization studies. In case of Tah18, we used the N-terminal part (first 972 of 2,286 bp/ first 324 of 761 amino acids) for localization.

Phaeodactylum tricornutum cells were transformed and positive transformants were cultured under standard conditions as described previously with 1.5 mM of NH_4Cl (Apt et al. 1996).

Fluorescence Microscopy

For in vivo localization the expression of the eGFP fusion proteins was induced with 0.9 mM of $NaNO_3$ for 2 days. The localization was visualized with a confocal laser scanning microscope Leica TCS SP2 using a HCX PL APO $40\times/1.25 - 0.75$ Oil CS objective. eGFP and chlorophyll fluorescence was excited at 488 nm. eGFP fluorescence was detected at a bandwidth of 500–520 nm and the chlorophyll (plastid autofluorescence) at a bandwidth of 625–720 nm, respectively. Pictures were processed with Fiji ImageJ with usage of BioFormats Importer plug-in (Linkert et al. 2010; Schindelin et al. 2012; Schneider et al. 2012; Rueden et al. 2017).

Results

Screening the Genomes of Cryptophytes, Chlorarachniophytes, and Diatoms for Components of a CIA Machinery

Cryptophytes, chlorarachniophytes, and diatoms possess a mitochondrion within the cytoplasm. As it was shown for important model systems such as yeast, this organelle exports a sulfur component which is used by the CIA machinery for the maturation of cytosolic and nuclear Fe–S proteins (Kispal et al. 2005; Srinivasan et al. 2014). Not surprisingly, our inspection of the available genome sequences highlighted genes for several cytosolic CIA factors, most likely targeted to the host-derived cytoplasms of *Guillardia theta* (cryptophyte), *Bigelowiella natans* (chlorarachniophytes), and *Phaeodactylum tricornutum* (diatom) (table 1 and supplementary table S1, Supplementary Material online).

In case a symbiont-specific CIA machinery is present in the PPC in parallel to a host version that is cytoplasmic, their factors should either be encoded by the nucleomorph genome within the PPC or by the nucleus genome of the host cell. In the latter case these factors should be equipped with a N-terminal targeting signal (bipartite targeting sequence, BTS; Gruber et al. 2007; Patron and Waller 2007) to ensure transport into the PPC. As exemplified for many PPC-located proteins of diatoms and cryptophytes, a typical PPC-specific BTS is composed of a signal peptide (SP) followed by a transit peptide-like (TPL) sequence, in which the first amino acid of

Table 1
Presence and Absence of CIA Factors in Cytosol and PPC

	Nbp35	Cfd1	Cia1	Cia2	Dre2	Nar1	Mms19	Tah18	Grx3	Grx4
Cytosol										
G. theta	+	+	+	+	+	+	n.d.	+	n.d.	+
B. natans	+	n.d.	+	+	+	+	+	n.d.	n.d.	+
P. tricornutum	+	n.d.	+	+	+	+	+	+	n.d.	+
PPC										
G. theta	+	n.d.	Nm	Nm	+	+	+	+	+	n.d.
B. natans	+	n.d.	n.d.	+	+	+	n.d.	+	n.d.	n.d.
P. tricornutum	n.d.	n.d.	n.d.	n.d.	n.d.	n.d.	n.d.	n.d.	n.d.	n.d.

+, factor present; n.d., factor not detected; Nm—Nucleomorph encoded.

the TPL is neither an aromatic amino acid nor a leucine (Gruber et al. 2007; Patron and Waller 2007). Although a BTS is present in the presequence of nucleus-encoded, PPC-directed proteins of chlorarachniophytes as well, a highly conserved amino acid at the first position of the TPL was not detected (Patron and Waller 2007). Using the absence/presence of a predicted BTS as a criterion, we identified CIA factors with a putative PPC destination for cryptophytes and chlorarachniophytes, as listed in table 1. Interestingly, we did not detect genes for PPC-directed Cia1 (a WD40 protein) and Cia2 (a MIP18 family-like motif harboring protein) factors in the nuclear genome of *Guillardia theta*. Instead, a reinspection of the nucleomorph genome sequence of the cryptophyte highlighted the two orfs, orf357 and orf143, respectively, most likely encoding the missing factors. The nucleomorph-encoded Cia1 and Cia2 candidate proteins show either a WD40-like motif and "Putative cytosolic iron–sulfur protein" prediction (Cia1, supplementary fig. S3, Supplementary Material online) or a MIP18 family-like motif and Fe–S cluster assembly (FSCA)' superfamily prediction (Cia2, supplementary fig. S4, Supplementary Material online), which strongly indicate the here proposed functions in the CIA targeting complex. For the distinction of Cfd1 and Nbp35 homologs a ferredoxin-like domain is indicative (e.g., Netz et al. 2016) which is present in the N-terminal regions of Nbp35- but not Cfd1-homologs. Using this criterion, we annotated the encoded proteins. Most notably, our screening confirms the finding of Tsaousis et al. (2014) in respect to the presence of a Cfd1-homolog in *G. theta*.

In case of the diatom *Phaeodactylum tricornutum*, the proteome of the PPC was already investigated in vivo (Moog et al. 2011). In this data set no potential Fe–S protein was identified. As a nucleomorph is absent in diatoms, no indications exist for the need of Fe–S proteins acting in the PPC. In agreement with the previous data, no CIA-factors with a PPC-specificity could be identified in in silico screens in the *P. tricornutum* genome (table 1).

For further analyses (see below), we reinspected the predicted gene models identified in the *G. theta* genome and included, if present, EST-data for correcting the gene models in some cases. This led to a promising data set of putative CIA

factors for the host and the symbiont (table 1 and supplementary table S1, Supplementary Material online). However, the BTS of the PPC-localized Tah18 of *G. theta* (supplementary fig. S1, Supplementary Material online) is predicted to be not very pronounced. The identification of CIA factors in the *B. natans* genome was more complicated due to the annotation of the genome. This was further complicated by the high intron load of the coding regions, missing EST-data covering the coding region and high levels of splice variants including both intron retention and exon skipping. Nevertheless, we identified several CIA factors (Nbp35, Nar1, Cia2, Dre2, and Tah18; table 1 and supplementary table S1, Supplementary Material online) in the *B. natans* genome, which are potentially PPC-localized, one of each with a putative BTS. However, in case of Dre2, Nbp35, and Tah18 the putative BTS is again not very pronounced.

Taken together, the in silico analyses indicated the presence of a CIA machinery in the PPCs of cryptophytes and most likely chlorarachniophytes, whereas evidence for such a machinery in the PPC of diatoms is absent.

Under the assumption that organisms having a transcriptionally active nucleomorph need a CIA machinery in their PPC, which is devoid of any traces of a mitochondrion, either a sulfur-component has to be imported for Fe–S cluster assembly or a NIF (nitrogen fixation)- or SUF-system (Lill and Muhlenhoff 2006; Stairs et al. 2014; Karnkowska et al. 2016;Freibert et al. 2017) should be present in this compartment. We have already postulated the presence of a SUF-system in cryptophytes, located in the stroma of their complex plastid (Hjorth et al. 2005), but found no indication of any SUF- or NIF-related factors with a PPC targeting signal in the genome of *G. theta*. Therefore, import of an activated sulfur component into the PPC, which is then used by a PPC-specific CIA machinery is likely. It is known from other eukaryotes that the mitochondria-localized ABC transporter Atm1 provides the cytoplasm with a sulfur component synthesized in the mitochondrion (e.g., Srinivasan et al. 2014). By scanning the genome of *G. theta* several potential ABC transporters were identified. One candidate shows, as expected, homology to Atm1 and a potential targeting signal for mitochondria (protein ID 188917). Aside from this canonical, most likely mitochondria localized version, other potential Atm1-like ABC transporters can be detected, but these have no striking similarity to Atm1. In addition, none of these candidates has a targeting signal for the outermost or second outermost membrane of the complex plastid. However, one of the putative ABC transporters from *G. theta* is predicted to be encoded as a preprotein having an N-terminal BTS with the specificity for the innermost plastid membrane (protein ID 164017).

In vivo Localization

For *G. theta* and *B. natans* transformation protocols are not established, preventing homologous expression of proteins in

these organisms. However, in earlier studies concerning the targeting signals of cryptophytes, we have shown that PPC-specific targeting sequences of *G. theta* perfectly direct proteins into the remnant cytoplasm of the secondary symbiont of the diatom *P. tricornutum* (Gould et al. 2006). Therefore, we localized the cryptophytic CIA factors heterologously, expressing a PPC targeting signal, fused to eGFP, in the diatom. This approach is especially important for the predicted PPC version of Tah18 from *G. theta*, which shows, as mentioned, a less-pronounced BTS-like structure at the N-terminus. We have expressed eGFP fusion proteins for the predicted CIA factors Nbp35, Nar1, Tah18, Dre2, and Grx3 (fig. 1). These fusion proteins localized within the PPC, as shown by a so-called blob-like structure of the eGFP signal (Kilian and Kroth 2005). Thus, the here predicted, PPC-specific CIA factors of cryptophytes are equipped with a targeting signal directing proteins into the PPC when heterologously expressed in the diatom system.

Phylogeny

In 2014, Tsaousis and colleagues published their results on the phylogeny of the CIA machinery in the stramenopile *Blastocystis* (Tsaousis et al. 2014). As an important outcome they demonstrated that the CIA machinery is uniquely found in eukaryotes. Although sequences from chlorarachniophytes, cryptophytes and diatoms were included into their study, only one copy of each CIA factor was integrated into the phylogenetic trees in the case of cryptophytes and chlorarachniophytes. Since we have shown here that a cytosolic and a PPC-located version of CIA factors are encoded in the genomes of *G. theta* and *B. natans*, we reinvestigated the phylogeny of the CIA factors Cfd1 and Nbp35. In addition, we incorporated our novel data on the localization of the CIA representatives when evaluating those results (fig. 2 and supplementary fig. S2, Supplementary Material online). Although Cfd1 and Nbp35 are homologous proteins, their sequences can be undoubtedly discerned due to a ferredoxin-like domain only present in the N-terminal region of Nbp35 proteins.

The phylogeny of Cfd1 and Nbp35 sequences including Hcf101 representatives (fig. 2 and supplementary fig. S2, Supplementary Material online) indicated, similar to the work of Tsaousis et al. (Tsaousis et al. 2014), a separation of the Cfd1 and Nbp35 branches. Sequences for the chloroplast-localized Hcf101 were integrated into the analyses since this protein, similar to Cfd1 and Nbp35, harbors a P-loop NTPase domain; Nar1 sequences served as outgroup to root the tree.

In case of the Nbp35 phylogeny, four clades were identified, an Opisthokonta-type, a plant-type and two SAR clades. Nbp35 of diatoms was found in one of the SAR clades (SAR-I), whereas in SAR-II the PPC and host Nbp35 versions of *B. natans* are grouping. Interestingly, the Nbp35 versions of *G. theta* branch differently, namely in case of the host version (nucleus-encoded, cytoplasmic) in the Opisthokonta clade

and, in case of the PPC version, together with red algal Nbp35 proteins in the plant-like clade. In case of Cfd1, we only found a host version for *G. theta*, which also has been shown before (Tsaousis et al. 2014), but none for *B. natans*. Similar to the host Nbp35 version, Cfd1 clusters in the Opisthokonta clade.

Discussion

Several ecologically and medically important organisms such as diatoms or the malaria causing protist *Plasmodium falciparum* harbor complex organized plastids that evolved from a phototrophic eukaryotic endosymbiont (e.g., Gould et al. 2008). Most of the compartments of the symbiont, such as the mitochondrion, were eliminated during coevolution of host and symbiont. However, intermediates in the extent of intracellular reduction of the phototrophic symbiont that has become a complex plastid are known. This is the case for chlorarachniophytes and cryptophytes, both of which harbor a plastid surrounded by four membranes (Maier et al. 2000). Here, the cytoplasm of the eukaryotic symbiont (PPC), is reduced in such a way that the nucleus of the former symbiont (nucleomorph) is in respect to size and coding capacity minimized (Douglas et al. 2001; Gilson et al. 2006; Lane et al. 2007; Tanifuji et al. 2011; Moore et al. 2012; Tanifuji et al. 2014a; Suzuki et al. 2015), but still present and active. However, the cellular reduction in others such as diatoms went further, so that for these organisms no cellular traces of a symbiotic nucleus were preserved. The morphological differences between organisms harboring a plastid surrounded by four membranes are manifested in several cell biological/biochemical functions; as shown here, this is also the case for CIA machineries, which are essential to assemble cytoplasmic iron–sulfur clusters for Fe–S proteins (fig. 3).

We have previously studied the PPC-proteome of the diatom *P. tricornutum* (Moog et al. 2011). This organism, as mentioned, has no nucleomorph and, as known so far, has only to manage a small set of cellular functions in the PPC, for which no Fe–S proteins seem to be essential. Consequently, no CIA machinery is necessary in the PPC of diatoms, which is supported by the in silico analyses presented here. Thus, our report indicates a eukaryotic (remnant) cytoplasm devoid of a CIA machinery. As known from other eukaryotes, several nucleus-located Fe–S proteins are acting in DNA replication, DNA repair, chromosome segregation and telomere length regulation (Rudolf et al. 2006; Netz et al. 2011; Gari et al. 2012; Stehling et al. 2012; Wu and Brosh 2012; Stehling et al. 2013; Paul and Lill 2015). Therefore, essentiality of Fe–S-clusters in at least some of these diatom proteins is expected and a CIA machinery should be expressed in the cytosol for the incorporation of Fe–S clusters into apo-proteins. Our screen for CIA factors supports this hypothesis. In addition, the CIA machinery of diatoms shows, by the lack of the factor Cfd1, a
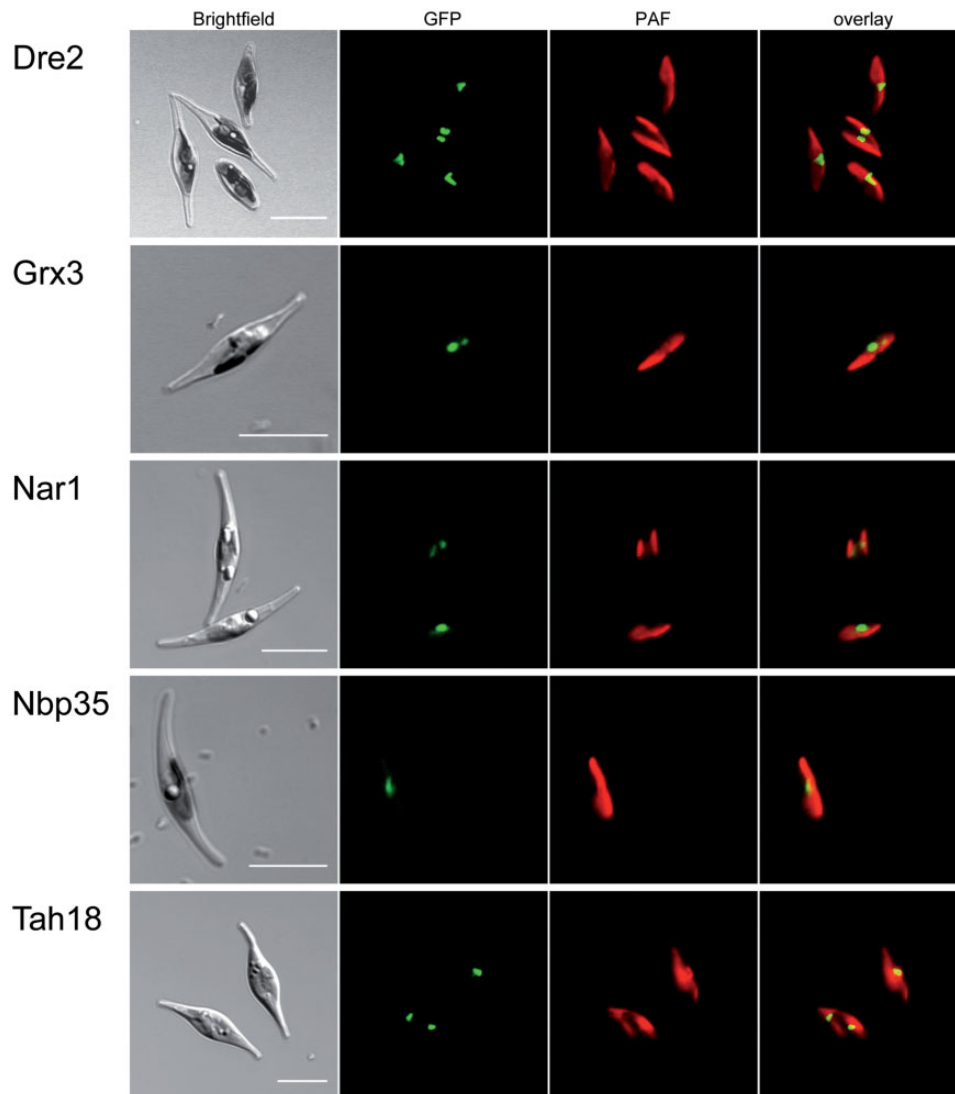
Fig. 1.—Heterologous localization of *G. theta* CIA factors in *P. tricornutum*. Potential PPC localized CIA factors of *G. theta* were heterologously expressed in *P. tricornutum* as GFP fusion proteins. Brightfield, GFP, plastid autofluorescence and overlay (from left to right) are shown. eGFP fluorescence shows a localization in a so-called blob-like structure which indicates a localization in the PPC. In the case of Dre2, Nar1 and Tah18 cells show two blob-like structures, indicating dividing cells. PAF: plastid autofluorescence. Scale Bar: 10 μm.

typical feature for a member of the SAR group (Tsaousis et al. 2014).

By knowing the importance of Fe–S proteins in genome maintenance and expression (Paul and Lill 2015), one has to postulate that nucleomorph-containing PPCs are depending on Fe–S proteins. In fact, according to our analyses, *B. natans* as well as *G. theta* might import putative Fe–S cluster apo-proteins into the PPC. In addition, an important Fe–S protein, Rli1, is encoded in the nucleomorph of *G. theta* (Douglas et al. 2001). Thus, cryptophytes and chlorarachniophytes should depend on a PPC-located CIA machinery. Our screen of the genomes of *G. theta* and *B. natans* genomes uncovered CIA factors equipped with a BTS besides those active in the cyto-sol. To verify that these factors are directed into a PPC, we performed in vivo localizations. As for *G. theta* and *B. natans* no transformation protocols are elaborated and therefore no in vivo localization experiments are possible, we studied tar-geting of the putative PPC-specific CIA factors in heterolo-gous localization experiments in the diatom system. This approach resulted in a localization of the eGFP-fusion proteins within the remnant cytoplasm of the eukaryotic symbiont in *P. tricornutum*, thereby confirming our in silico predictions in a heterologous system (fig. 1).

Altogether, the here described PPC-specific CIA factors encoded in the nuclear genome of *G. theta* make up a nearly complete machinery known from studies in other organisms (fig. 3). Missing factors apparently not encoded in the nuclear genome of the cryptophyte are Cia1 and Cia2, which are part
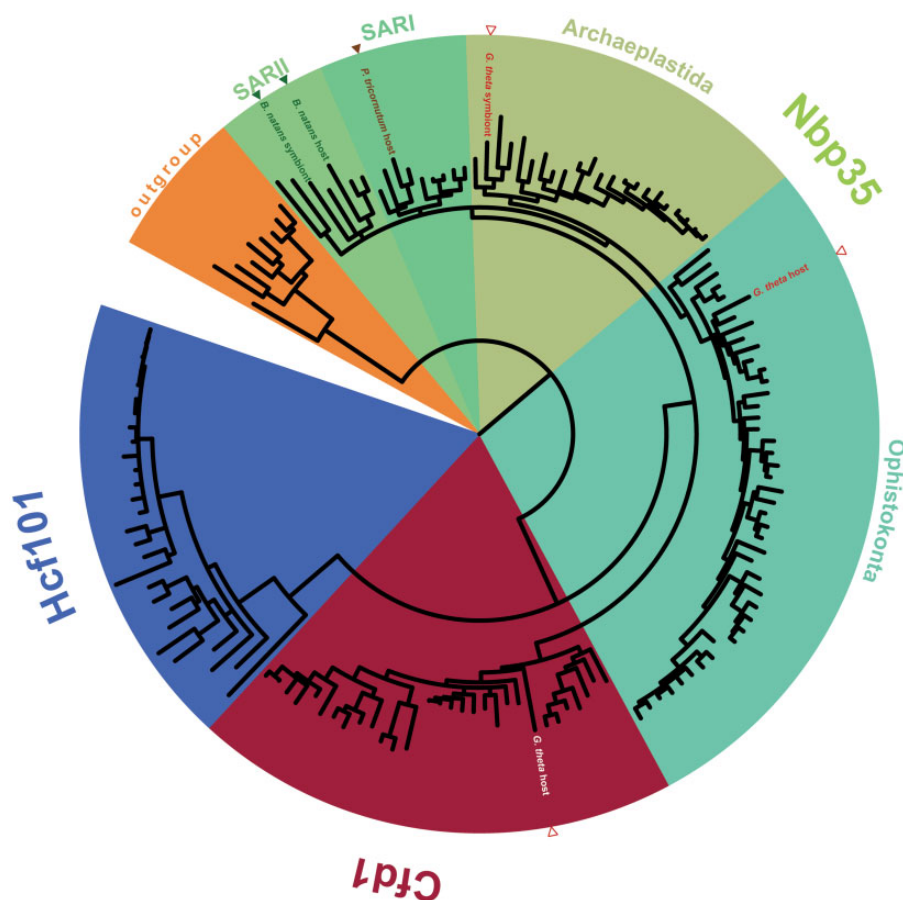
Fig. 2.—Schematic representation of phylogeny of Cfd1 and Nbp35. The main clades of Nbp35 (green), Cfd1 (red), and Hcf101 (blue) are shown. Host (cytosol) and symbiont (PPC) specific copies of Nbp35 and Cfd1 are highlighted for *B. natans*, *G. theta* and *P. tricornutum* in green, red/white, and brown, respectively. In contrast to *B. natans* and *P. tricornutum*, *G. theta* encodes a host-specific Cfd1. *G. theta* Nbp35 host and symbiont proteins cluster in the *Archaeplastida* and *Ophistokonta* clades, whereas both *B. natans* proteins reside in the SAR clade.

of the so-called targeting complex responsible for the transfer of Fe–S clusters on target apo-proteins (Balk and Lobreaux 2005; Srinivasan et al. 2007; Stehling and Lill 2013). However, in *G. theta* these factors seem to be encoded in the nucleomorph genome, previously annotated as Orf357 and Orf143 (Douglas et al. 2001). Although the sequence similarity of these Orfs to nuclear-encoded Cia1 and Cia2 versions of other organisms is low, the presence of indicative domains supports their identity as factors of the CIA machinery (supplementary figs. S3 and S4, Supplementary Material online). This is not restricted to *G. theta*, because the nucleomorph of *Chroomonas mesostigmatica*, *Cryptomonas paramecium* and *Hemiselmis andersenii* (Lane et al. 2007; Tanifuji et al. 2011; Moore et al. 2012) encode these orfs as well. Therefore, the here presented data support the conclusion that a complete set of CIA factors is present in the PPC of the cryptophyte *G. theta* (fig. 3). Although not proven in respect to the localization of the factors, our data indicate the presence of a second, PPC-located CIA machinery for *B. natans* as well.

These results, together with earlier findings on the absence of a PPC-located mitochondrion, raise the question on the origin of a sulfur component necessary for Fe–S cluster assembly by the PPC-specific CIA machinery in cryptophytes. Fe–S clusters can be synthesized not only by an ISC machinery, but also by a SUF- or NIF-machinery. A SUF-machinery was indeed described for cryptophytes, but it is localized within the stroma (Hjorth et al. 2005). To pursue the hypothesis of a putative PPC-located NIF-machinery an in silico screening for NIF-specific factors was performed. However, no matches were found (data not shown). Thus, we predict that an activated sulfur component for ISC synthesis is imported into the PPC, which is in principle possible either from the host-derived cytoplasm or the stroma. In the case that the activated sulfur component stems from the host, two membranes have to be crossed, similar to an origin of the component in the stroma, where an active transport across the innermost and second innermost membrane of the plastid is required.

In order to investigate the origin of the sulfur component for Fe–S cluster synthesis in cryptophytes, we searched for
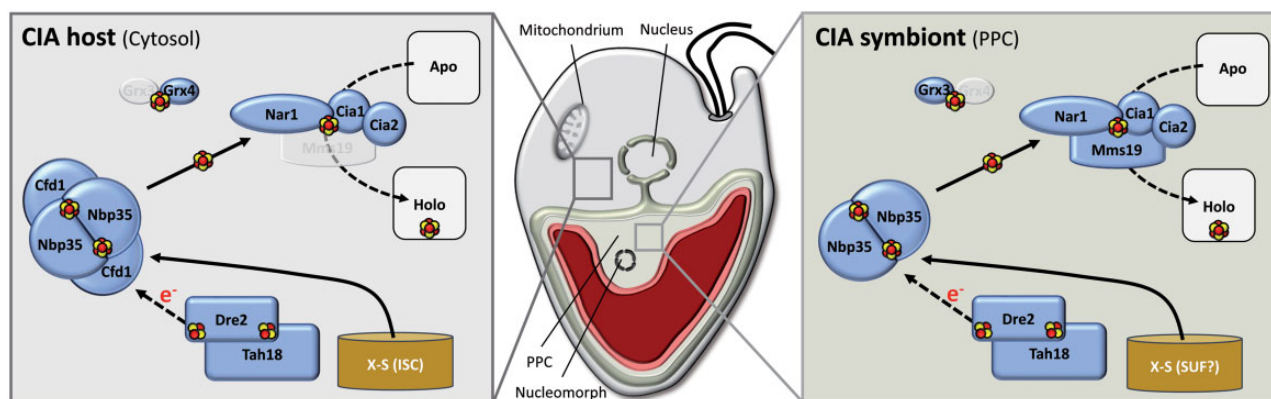
Fig. 3.—Two different CIA machineries in *Guillardia theta*. Host (cytosol) and symbiont (PPC) specific version of cytosolic iron–sulfur protein assembly (CIA) machineries are shown schematically. The cytosolic CIA machinery builds iron–sulfur clusters and is dependent on a so far not identified sulfur component (X-S) provided by the mitochondrial ISC. In case of PPC located CIA this X-S may be provided by the plastidal SUF machinery. Identified factors are shown in blue, factors which could not be identified are shown in transparent. Red/yellow spheres represent [4Fe–4S] and [2Fe–2S] clusters. Nbp35/Cfd1 or Npb35 multimers are scaffolds for iron–sulfur Cluster formation and their function is dependent on [4Fe–4S] cluster binding. In turn, the maturation of these multimers is dependent on the electron transfer system build by Tah18–Dre2, the latter also complexed with [2Fe–2S] clusters. Apo-proteins are loaded with iron–sulfur clusters via Nar1 by the Mms19-Cia1-Cia2 targeting complex. Grx3/Grx4 have been shown to be involved in iron–sulfur cluster formation but their precise role is not fully understood. Possibly, only one Grx is present in the cytosol and the PPC of *G. theta*.

Atm1 homologs. This mitochondrial ABC transporter was shown to export a sulfur component used by the cytosolic CIA machinery (e.g., Kispal et al. 1999; reviewed in Lill et al. 2014). Although several ABC transporters are encoded by the *G. theta* genome, the ones with the highest sequence similarities are a predicted mitochondrial version of Atm1 and another predicted to be localized in a plastid membrane. The nature of the latter is not really indicative due to a generally high primary sequence conservation of ABC transporters. Nevertheless, we propose that the sulfur component used by the PPC-located CIA machinery of *G. theta* is synthesized by a SUF system of the complex plastid and exported from the plastid stroma into the PPC via an ABC transporter in the inner plastid membrane (fig. 3). Although the origin of a SUF-depending sulfur component used by a CIA machinery might be unusual, examples for that are known. Especially in the case of *Monocercomonoides* sp. (Karnkowska et al. 2016), a protist synthesizing Fe–S clusters by a laterally acquired bacterial SUF system, which is, however, acting in the host-derived cytosol.

The evolution of organisms with complex plastids of red algal origin ("chromalveolates", Cavalier-Smith 1999) is still a matter of debate and a monophyletic or even higher order origin have been proposed (Cavalier-Smith 1999; Burki et al. 2012; Gould et al. 2015, and references therein). However, it is accepted by most scientists that the plastid of chromalveolates is of red algal origin. In any case, the evolution of the chromalveolates cannot be deciphered by investigating the symbiont only. Therefore, the host genome might be informative, especially with regard to the presence of genes encoding for components of the core metabolism such as

Fe–S cluster synthesis. In case of a CIA machinery, the scaffold for iron–sulfur protein assembly shows a specific protein composition. The central component for this scaffold is Nbp35, which interacts, according to the molecular analyses in yeast and human, with Cfd1 (e.g., Lill et al. 2015). Nevertheless, a recent report indicates that Nbp35 of *Arabidopsis* interacts with Dre2, another conserved component of the CIA machinery (Bastow et al. 2017). Cfd1 is encoded in Amoebozoa, ascomycetes, basidiomycetes, metazoans and others, but is generally absent in Archaeplastida and the SAR group (Tsaousis et al. 2014). Thus, the presence or absence of Cfd1 might be an informative character at least for the evolution of chromalveolates. In this respect the presence of Cfd1 in cryptophytes in combination with several other recent studies might indicate a complex evolution of cryptophytes, which differs from that of other chromalveolates (figs. 2 and 3 and supplementary fig. S2, Supplementary Material online) (e.g., Bachvaroff et al. 2005; Bodył 2005; Teich et al. 2007; Burki et al. 2012; Petersen et al. 2014; Stiller et al. 2014). If this statement is correct, other CIA factors should show a non-chromalveolate grouping in phylogenies as well when cryptophytic factors are compared with homologs of the Archaeplastida and the SAR. This was indeed seen in respect to Nbp35. As shown in figure 2, representatives of Nbp35 group in one of the four Nbp35 clades, two of which are specific either for Opisthokonta or Archaeplastida. The third and fourth group (the SAR group I and SAR group II) include the diatom Nbp35 (SAR group I) whereas the PPC and host version of the chlorarachniophyte *B. natans* are members of the SAR group II clade. In contrast, the cryptophytic Nbp35 proteins group with the Opisthokonta (host Nbp35) and in the

Archaeplastida branch close to red algae, as expected for the PPC version of Nbp35. Therefore, the cryptophytic host CIA machinery differs from the SAR group CIA systems not only in the presence of a Cfd1, but also in the inferred phylogenetic origin for Nbp35.

As mentioned, both Nbp35 of *B. natans* cluster in SAR group II. This might indicate that they have been subject to a duplication event. Complex plastids of chlorarachniophytes like *B. natans* are thought to have evolved from green algae ancestors (e.g., Curtis et al. 2012). Therefore, we rather would have expected one of these Nbp35s to cluster within Archaeplastida, comparable to the situation seen in *G. theta*. In case of a duplication event, the host version (SAR) might have been duplicated and have been equipped with a suitable BTS for PPC targeting. With this, the symbiont version of Nbp35 was not needed anymore and got lost.

We recently inspected the origin of several nucleus-encoded factors directed into the complex plastid of diatoms and other chromalveolates like SELMA (symbiont-specific ERAD-like machinery) and triosephosphate transporters (Hempel et al. 2009; Felsner et al. 2011; Moog et al. 2015). Our phylogenetic analyses revealed that these components, located in the PPCs and plastid membranes of chromalveolates, are of symbiont (red algal) origin. Interestingly, this is also the case with respect to the PPC-specific CIA factor Nbp35 in cryptophytes, indicating that although a host copy is present, the symbiont version of Nbp35 is of cell biological/biochemical importance and is maintained as long as they are needed. However, the situation is different in respect to predicted Nbp35 PPC version of *B. natans*, which is grouping in the SAR group and not together with green alga/land plants. A similar result was shown in the work of Hopkins et al. (2012), indicating that several PPC and stroma targeted proteins are of nongreen origin.

Conclusions

Taken together the here reported phylogenetic study of Nbp35 and the presence of a Cfd1 factor in *G. theta* suggest that cryptophytes are cellular mergers, which originated by the union of a red alga and a host cell, the latter with a different phylogenetic origin than in other members of the chromalveolates. More than a speculation is our finding that a PPC-specific CIA machinery correlates with the presence of a nucleomorph. Nevertheless, cryptophytes have a PPC-specific iron–sulfur burden, which necessitates a CIA machinery presumably fed by a sulfur component synthesized in the stroma.

Supplementary Material

Supplementary data are available at *Genome Biology and Evolution* online.

Literature Cited

Altschul SF, Gish W, Miller W, Myers EW, Lipman DJ. 1990. Basic local alignment search tool. J Mol Biol. 215(3):403–410.

Apt KE, Kroth-Pancic PG, Grossman AR. 1996. Stable nuclear transformation of the diatom *Phaeodactylum tricornutum*. Mol Gen Genet. 252(5):572–579.

Bachvaroff TR, Sanchez Puerta MV, Delwiche CF. 2005. Chlorophyll c-containing plastid relationships based on analyses of a multigene data set with all four chromalveolate lineages. Mol Biol Evol. 22(9):1772–1782.

Balk J, Lobreaux S. 2005. Biogenesis of iron–sulfur proteins in plants. Trends Plant Sci. 10(7):324–331.

Balk J, Pilon M. 2011. Ancient and essential: the assembly of iron–sulfur clusters in plants. Trends Plant Sci. 16(4):218–226.

Bastow EL, Bych K, Crack JC, Le Brun NE, Balk J. 2017. NBP35 interacts with DRE2 in the maturation of cytosolic iron–sulphur proteins in *Arabidopsis thaliana*. Plant J. 89(3):590–600.

Bendtsen JD, Nielsen H, von Heijne G, Brunak S. 2004. Improved prediction of signal peptides: signalP 3.0. J Mol Biol. 340(4):783–795.

Bernard DG, Cheng Y, Zhao Y, Balk J. 2009. An allelic mutant series of ATM3 reveals its key role in the biogenesis of cytosolic iron–sulfur proteins in Arabidopsis. Plant Physiol. 151(2):590–602.

Bodył A. 2005. Do plastid-related characters support the Chromalveolate hypothesis?. J Phycol. 41(3):712–719.

Bolte K, et al. 2009. Protein targeting into secondary plastids. J Eukaryot Microbiol. 56(1):9–15.

Bowler C, et al. 2008. The Phaeodactylum genome reveals the evolutionary history of diatom genomes. Nature 456(7219):239–244.

Burki F, Okamoto N, Pombert JF, Keeling PJ. 2012. The evolutionary history of haptophytes and cryptophytes: phylogenomic evidence for separate origins. Proc Biol Sci. 279(1736):2246–2254.

Cavalier-Smith T. 1999. Principles of protein and lipid targeting in secondary symbiogenesis: euglenoid, dinoflagellate, and sporozoan plastid origins and the eukaryote family tree. J Eukaryot Microbiol. 46(4):347–366.

Clamp M, Cuff J, Searle SM, Barton GJ. 2004. The Jalview Java alignment editor. Bioinformatics 20(3):426–427.

Curtis BA, et al. 2012. Algal genomes reveal evolutionary mosaicism and the fate of nucleomorphs. Nature 492(7427):59–65.

Darriba D, Taboada GL, Doallo R, Posada D. 2011. ProtTest 3: fast selection of best-fit models of protein evolution. Bioinformatics 27(8):1164–1165.

Dawson NL, et al. 2017. CATH: an expanded resource to predict protein function through structure and sequence. Nucleic Acids Res. 45(D1):D289–D295.

Douglas S, et al. 2001. The highly reduced genome of an enslaved algal nucleus. Nature 410(6832):1091–1096.

Edgar RC. 2004. MUSCLE: multiple sequence alignment with high accuracy and high throughput. Nucleic Acids Res. 32(5):1792–1797.

Emanuelsson O, Nielsen H, Brunak S, von Heijne G. 2000. Predicting subcellular localization of proteins based on their N-terminal amino acid sequence. J Mol. Biol. 300(4):1005–1016.

Felsner G, et al. 2011. ERAD components in organisms with complex red plastids suggest recruitment of a preexisting protein transport pathway for the periplastid membrane. Genome Biol Evol. 3:140–150.

Finn RD, et al. 2015. HMMER web server: 2015 update. Nucleic Acids Res. 43(W1):W30–W38.

Freibert SA, et al. 2017. Evolutionary conservation and in vitro reconstitution of microsporidian iron–sulfur cluster biosynthesis. Nat Commun. 8:13932.

Gari K, et al. 2012. MMS19 links cytoplasmic iron–sulfur cluster assembly to DNA metabolism. Science 337(6091):243–245.

Gilson PR, et al. 2006. Complete nucleotide sequence of the chlorarachniophyte nucleomorph: nature's smallest nucleus. Proc Natl Acad Sci U S A. 103(25):9566–9571.

Gould SB, Maier UG, Martin WF. 2015. Protein import and the origin of red complex plastids. Curr Biol. 25(12):R515–R521.

Gould SB, et al. 2006. Protein targeting into the complex plastid of cryptophytes. J Mol Evol. 62(6):674–681.

Gould SB, Waller RF, McFadden GI. 2008. Plastid evolution. Annu Rev Plant Biol. 59:491–517.

Grosche C, Funk HT, Maier UG, Zauner S. 2012. The chloroplast genome of *Pellia endiviifolia*: gene content, RNA-editing pattern, and the origin of chloroplast editing. Genome Biol Evol. 4(12):1349–1357.

Grosche C, Hempel F, Bolte K, Zauner S, Maier UG. 2014. The periplastidal compartment: a naturally minimized eukaryotic cytoplasm. Curr Opin Microbiol. 22:88–93.

Gruber A, et al. 2007. Protein targeting into complex diatom plastids: functional characterisation of a specific targeting motif. Plant Mol Biol. 64(5):519–530.

Guillard RRL. 1975. Culture of phytoplankton for feeding marine invertebrates. In: Smith WL, Chanley MH, editors. Culture of marine invertebrate animals. Proceedings—1st Conference on Culture of Marine Invertebrate Animals Greenport; Boston, MA: Springer US. p. 29–60.

Guindon S, Gascuel O. 2003. A simple, fast, and accurate algorithm to estimate large phylogenies by maximum likelihood. Syst Biol. 52(5):696–704.

Hempel F, et al. 2007. Transport of nuclear-encoded proteins into secondarily evolved plastids. Biol Chem. 388(9):899–906.

Hempel F, Bullmann L, Lau J, Zauner S, Maier UG. 2009. ERAD-derived preprotein transport across the second outermost plastid membrane of diatoms. Mol Biol Evol. 26(8):1781–1790.

Hjorth E, Hadfi K, Zauner S, Maier UG. 2005. Unique genetic compartmentalization of the SUF system in cryptophytes and characterization of a SufD mutant in *Arabidopsis thaliana*. FEBS Lett. 579(5):1129–1135.

Hopkins JF, et al. 2012. Proteomics reveals plastid- and periplastid-targeted proteins in the chlorarachniophyte alga *Bigelowiella natans*. Genome Biol Evol. 4(12):1391–1406.

Karnkowska A, et al. 2016. A eukaryote without a mitochondrial organelle. Curr Biol. 26(10):1274–1284.

Kilian O, Kroth PG. 2005. Identification and characterization of a new conserved motif within the presequence of proteins targeted into complex diatom plastids. Plant J. 41(2):175–183.

Kispal G, Csere P, Prohl C, Lill R. 1999. The mitochondrial proteins Atm1p and Nfs1p are essential for biogenesis of cytosolic Fe/S proteins. EMBO J. 18(14):3981–3989.

Kispal G, et al. 2005. Biogenesis of cytosolic ribosomes requires the essential iron–sulphur protein Rli1p and mitochondria. EMBO J. 24(3):589–598.

Kushnir S, et al. 2001. A mutation of the mitochondrial ABC transporter Sta1 leads to dwarfism and chlorosis in the Arabidopsis mutant starik. Plant Cell 13(1):89–100.

Lane CE, et al. 2007. Nucleomorph genome of *Hemiselmis andersenii* reveals complete intron loss and compaction as a driver of protein structure and function. Proc Natl Acad Sci U S A. 104(50):19908–19913.

Letunic I, Bork P. 2016. Interactive tree of life (iTOL) v3: an online tool for the display and annotation of phylogenetic and other trees. Nucleic Acids Res. 44(W1):W242–W245.

Lewis TE, et al. 2018. Gene3D: extensive prediction of globular domains in proteins. Nucleic Acids Res. 46(D1):D1282.

Lill R, et al. 2015. The role of mitochondria and the CIA machinery in the maturation of cytosolic and nuclear iron–sulfur proteins. Eur J Cell Biol. 94(7-9):280–291.

Lill R, et al. 2012. The role of mitochondria in cellular iron–sulfur protein biogenesis and iron metabolism. Biochim Biophys Acta 1823(9):1491–1508.

Lill R, Muhlenhoff U. 2006. Iron–sulfur protein biogenesis in eukaryotes: components and mechanisms. Annu Rev Cell Dev Biol. 22:457–486.

Lill R, Srinivasan V, Muhlenhoff U. 2014. The role of mitochondria in cytosolic-nuclear iron–sulfur protein biogenesis and in cellular iron regulation. Curr Opin Microbiol. 22:111–119.

Linkert M, et al. 2010. Metadata matters: access to image data in the real world. J Cell Biol. 189(5):777–782.

Maier UG, Douglas SE, Cavalier-Smith T. 2000. The nucleomorph genomes of cryptophytes and chlorarachniophytes. Protist 151(2):103–109.

Maier UG, Zauner S, Hempel F. 2015. Protein import into complex plastids: cellular organization of higher complexity. Eur J Cell Biol. 94(7-9):340–348.

Maier UG, et al. 2013. Massively convergent evolution for ribosomal protein gene content in plastid and mitochondrial genomes. Genome Biol Evol. 5(12):2318–2329.

Makiuchi T, Nozaki T. 2014. Highly divergent mitochondrion-related organelles in anaerobic parasitic protozoa. Biochimie 100:3–17.

Moog D, Rensing SA, Archibald JM, Maier UG, Ullrich KK. 2015. Localization and evolution of putative triose phosphate translocators in the diatom *Phaeodactylum tricornutum*. Genome Biol Evol. 7(11):2955–2969.

Moog D, Stork S, Zauner S, Maier UG. 2011. In silico and in vivo investigations of proteins of a minimized eukaryotic cytoplasm. Genome Biol Evol. 3:375–382.

Moore CE, Archibald JM. 2009. Nucleomorph genomes. Annu Rev Genet. 43:251–264.

Moore CE, Curtis B, Mills T, Tanifuji G, Archibald JM. 2012. Nucleomorph genome sequence of the cryptophyte alga *Chroomonas mesostigmatica* CCMP1168 reveals lineage-specific gene loss and genome complexity. Genome Biol Evol. 4(11):1162–1175.

Mühlenhoff U, et al. 2015. Compartmentalization of iron between mitochondria and the cytosol and its regulation. Eur J Cell Biol. 94(7–9):292–308.

Netz DJ, et al. 2016. The conserved protein Dre2 uses essential [2Fe–2S] and [4Fe–4S] clusters for its function in cytosolic iron–sulfur protein assembly. Biochem J. 473(14):2073–2085.

Netz DJ, Mascarenhas J, Stehling O, Pierik AJ, Lill R. 2014. Maturation of cytosolic and nuclear iron–sulfur proteins. Trends Cell Biol. 24(5):303–312.

Netz DJ, et al. 2011. Eukaryotic DNA polymerases require an iron–sulfur cluster for the formation of active complexes. Nat Chem Biol. 8(1):125–132.

Nurenberg E, Tampe R. 2013. Tying up loose ends: ribosome recycling in eukaryotes and archaea. Trends Biochem Sci. 38(2):64–74.

Patron NJ, Waller RF. 2007. Transit peptide diversity and divergence: a global analysis of plastid targeting signals. Bioessays 29(10):1048–1058.

Paul VD, Lill R. 2015. Biogenesis of cytosolic and nuclear iron–sulfur proteins and their role in genome stability. Biochim Biophys Acta 1853(6):1528–1539.

Petersen J, et al. 2014. *Chromera velia*, endosymbioses and the rhodoplex hypothesis—plastid evolution in cryptophytes, alveolates, stramenopiles, and haptophytes (CASH lineages). Genome Biol Evol. 6(3):666–684.

Potter SC, et al. 2018. HMMER web server: 2018 update. Nucleic Acids Res. 46(W1):W200–W204.

Ronquist F, et al. 2012. MrBayes 3.2: efficient Bayesian phylogenetic inference and model choice across a large model space. Syst Biol. 61(3):539–542.

Rost B. 1999. Twilight zone of protein sequence alignments. Protein Eng. 12(2):85–94.

Rudolf J, Makrantoni V, Ingledew WJ, Stark MJ, White MF. 2006. The DNA repair helicases XPD and FancJ have essential iron–sulfur domains. Mol Cell 23(6):801–808.

Rueden CT, et al. 2017. ImageJ2: ImageJ for the next generation of scientific image data. BMC Bioinformatics 18(1):529.

Schindelin J, et al. 2012. Fiji: an open-source platform for biological-image analysis. Nat Methods 9(7):676–682.

Schneider CA, Rasband WS, Eliceiri KW. 2012. NIH Image to ImageJ: 25 years of image analysis. Nat Methods 9(7):671–675.

Srinivasan V, et al. 2007. Structure of the yeast WD40 domain protein Cia1, a component acting late in iron–sulfur protein biogenesis. Structure 15:1246–1257.

Srinivasan V, Pierik AJ, Lill R. 2014. Crystal structures of nucleotide-free and glutathione-bound mitochondrial ABC transporter Atm1. Science 343(6175):1137–1140.

Stairs CW, et al. 2014. A SUF Fe–S cluster biogenesis system in the mitochondrion-related organelles of the anaerobic protist Pygsuia. Curr Biol. 24(11):1176–1186.

Stehling O, Lill R. 2013. The role of mitochondria in cellular iron–sulfur protein biogenesis: mechanisms, connected processes, and diseases. Cold Spring Harb Perspect Biol. 5(8):a011312.

Stehling O, et al. 2013. Human CIA2A-FAM96A and CIA2B-FAM96B integrate iron homeostasis and maturation of different subsets of cytosolic-nuclear iron–sulfur proteins. Cell Metab. 18(2):187–198.

Stehling O, et al. 2012. MMS19 assembles iron–sulfur proteins required for DNA metabolism and genomic integrity. Science 337(6091):195–199.

Stehling O, Wilbrecht C, Lill R. 2014. Mitochondrial iron–sulfur protein biogenesis and human disease. Biochimie 100:61–77.

Stiller JW, et al. 2014. The evolution of photosynthesis in chromist algae through serial endosymbioses. Nat Commun. 5:5764.

Strunk BS, Novak MN, Young CL, Karbstein K. 2012. A translation-like cycle is a quality control checkpoint for maturing 40S ribosome subunits. Cell 150(1):111–121.

Suzuki S, Ishida K, Hirakawa Y. 2016. Diurnal transcriptional regulation of endosymbiotically derived genes in the chlorarachniophyte *Bigelowiella natans*. Genome Biol Evol. 8(9):2672–2682.

Suzuki S, Shirato S, Hirakawa Y, Ishida K. 2015. Nucleomorph genome sequences of two *Chlorarachniophytes*, *Amorphochlora amoebiformis* and *Lotharella vacuolata*. Genome Biol Evol. 7(6):1533–1545.

Tanifuji G, et al. 2014. Nucleomorph and plastid genome sequences of the chlorarachniophyte *Lotharella oceanica*: convergent reductive evolution and frequent recombination in nucleomorph-bearing algae. BMC Genomics 15(1):374.

Tanifuji G, Onodera NT, Moore CE, Archibald JM. 2014. Reduced nuclear genomes maintain high gene transcription levels. Mol Biol Evol. 31(3):625–635.

Tanifuji G, et al. 2011. Complete nucleomorph genome sequence of the nonphotosynthetic alga *Cryptomonas paramecium* reveals a core nucleomorph gene set. Genome Biol Evol. 3:44–54.

Teich R, Zauner S, Baurain D, Brinkmann H, Petersen J. 2007. Origin and distribution of Calvin cycle fructose and sedoheptulose bisphosphatases in plantae and complex algae: a single secondary origin of complex red plastids and subsequent propagation via tertiary endosymbioses. Protist 158(3):263–276.

Tsaousis AD, Gentekaki E, Eme L, Gaston D, Roger AJ. 2014. Evolution of the cytosolic iron–sulfur cluster assembly machinery in Blastocystis species and other microbial eukaryotes. Eukaryot Cell 13(1):143–153.

Wu Y, Brosh RM Jr. 2012. DNA helicase and helicase-nuclease enzymes with a conserved iron–sulfur cluster. Nucleic Acids Res. 40(10):4247–4260.

Associate editor: Martin Embley